Mollow sidebands in high order harmonic spectra of molecules

Yuqing Xia and Agnieszka Jaron-Becker*

JILA and Department of Physics, University of Colorado at Boulder, Boulder, Colorado 80309-0440, USA

*jaron@jila.colorado.edu

Abstract: Novel feature of high order harmonic generation process for molecules is presented for several molecules at their equilibrium geometries. The high order harmonic spectra reveal additional sidebands for each odd harmonic, which are a consequence of the resonant coupling of two valence orbitals, a mechanism analogous to Mollow triplets known from quantum optics. Strong modification of the high order harmonic generation process is illustrated with time frequency analysis in which there appear additional minima dependent on the Rabi frequency for the corresponding transition. The orbital coupling further leads to the modification of the electron dynamics which is presented using total electron density difference maps.

OCIS codes: (020.2649) Strong field laser physics; (020.4180) Multiphoton physics; (191.4190) Multiphoton processes; (190,7110) Ultrafast nonlinear optics; (190.4160) Multiharmonic generation.

References and links

1. A. McPherson, G. Gibson, H. Jara, T. S. Luk, I. A. McIntyre, K. Boyer, and C. K. Rhodes,"Studies of Multiphoton Production of Vacuum Ultraviolet Radiation in the Rare Gase," J. Opt. Soc. Am. B **4**, 595–601 (1987).
2. M. Ferray, A. L'Huillier, X.F. Li, L.A. Lompre, G. Mainfray, and C. Manus, "Multiple-harmonic conversion of 1064 nm radiation in rare gases," J. Phys. B: At. Mol. Opt. Phys. **21**, L31–L35 (1988).
3. T. Popmintchev, M.-C. Chen, D. Popmintchev, P. Arpin, S. Brown, S. Alisauskas, G. Andriukaitis, T. Balciunas, O.D. Mücke, A. Pugzlys, A. Baltuska, B. Shim, S. E. Schrauth, A. Gaeta, C. Hernandez-Garcia, L. Plaja, A. Becker, A. Jaron-Becker, M. M. Murnane, and H. C. Kapteyn,"Bright Coherent Ultrahigh Harmonics in the keV X-ray Regime from Mid-Infrared Femtosecond Lasers," Science **91**, 1287–1291 (2012).
4. I. P. Christov, M. M. Murnane and H. C. Kapteyn, "High-Harmonic Generation of Attosecond Pulses in the 'Single-Cycle' Regime," Phys. Rev. Lett. **78**, 1251–1254 (1997).
5. M. Hentschel, R. Kienberger, Ch. Spielmann, G. A. Reider, N. Milosevic, T. Brabec, P. Corkum, U. Heinzmann, M. Drescher, and F. Krausz, "Attosecond metrology," Nature **414**, 509–513 (2001).
6. P. M. Paul, E. S. Toma, P. Breger, G. Mullot, F. Auge, Ph. Balcou, H. G. Muller, and P. Agostini, "Observation of a Train of Attosecond Pulses from High Harmonic Generation," Science **292**, 1689–1692 (2001).
7. M.-C. Chen, C. Mancuso, C. Hernandez-Garcia, F. Dollar, B. Galloway, D. Popmintchev, P.-C. Huang, B. Walker, L. Plaja, A. A. Jaron-Becker, A. Becker, M. M. Murnane, H. C. Kapteyn, and T. Popmintchev, "Generation of bright isolated attosecond soft X-ray pulses driven by multicycle midinfrared lasers," Proc. Nat. Acad. Sciences U.S.A. **111**, E2361–E2367 (2014).
8. D. Popmintchev, C. Hernandez-Garcia, F. Dollar, C. Mancuso, J. Perez-Hernndez, M. C. Chen, A. Hankla, X. Gao, B. Shim, A. Gaeta, M. Tarazkar, D. Romanov, R. Levis, J. Gaffney, M. Foord, S. Libby, A. Jaron-Becker, A. Becker, L. Plaja, M. Murnane, H. Kapteyn, T. Popmintchev, "Efficient soft X-ray high harmonic generation in multiply- ionized plasmas: the ultraviolet surprise," Science **350** 1225–123131 (2015).
9. I. Lopez-Quintas, M. Oujja, M. Sanz, M. Martin, R. A. Ganeev, and M. Castillejo, "Low-order harmonic generation in nanosecond laser ablation plasmas of carbon containing materials," Appl. Surf. Sci. **278** 33–37 (2013).
10. M. Lein, "Molecular imaging using recolliding electrons," J. Phys. B: At. Mol. Opt. Phys. **40**, R135–R173 (2007).

#255420 Received 9 Dec 2015; revised 23 Jan 2016; accepted 26 Jan 2016; published 25 Feb 2016

11. X. B. Zhou, R. Lock, W. Li, N. Wagner, M. M. Murnane, and H. C. Kapteyn, "Molecular Recollision Interferometry in High Harmonic Generation," Phys. Rev. Lett. **100**, 073902 (2008).
12. W. Boutu, S. Haessler, H. Merdji, P. Breger, G. Waters, M. Stankiewicz, L. J. Frasinski, R. Taieb, J. Caillat, A. Maquet, P. Monchicourt, B. Carre, and P. Salieres, "Coherent control of attosecond emission from aligned molecules," Nat. Phys. **4**, 545–549 (2008).
13. W. Li, X. Zhou, R. Lock, S. Patchkovskii, A. Stolow, H. C. Kapteyn, and M. M. Murnane, "Time-Resolved Dynamics in N_2O_4 Probed Using High Harmonic Generation," Science **322**, 1207–1211 (2008).
14. O. Smirnova, Y. Mairesse, S. Patchkovskii, N. Dudovich, D. Villeneuve, P. Corkum, and M. Yu. Ivanov, "High harmonic interferometry of multi-electron dynamics in molecules," Nature **460**, 972–977 (2009).
15. H. J. Wörner, J. B. Bertrand, D. V. Kartashov, P. B. Corkum, and D. M. Villeneuve, "Following a chemical reaction using high-harmonic interferometry," Nature **466**, 604–607 (2010).
16. C. Vozzi, C. Negro, F. Calegari, G. Sansone, M. Nisoli, S. DeSilvestri, and S. Stagira, "Generalized molecular orbital tomography," Nat. Phys. **7**, 822–826 (2011).
17. P. B. Corkum, "Plasma perspective on strong field multiphoton ionization," Phys. Rev. Lett. **71**, 1994–1998 (1993).
18. Y. Mairesse, J. Higuet, N. Dudovich, D. Shafir, B. Fabre, E. Mevel, E. Constant, S. Patchkovskii, Z. Walters, M.Yu. Ivanov, and O. Smirnova, "High harmonic spectroscopy of multichannel dynamics in strong-field ionization," Phys. Rev. Lett. **104**, 213601 (2010).
19. A.-T. Le, R. R. Lucchese, and C. D. Lin, "Polarization and ellipticity of high-order harmonics from aligned molecules generated by linearly polarized intense laser pulses," Phys. Rev. A **82**, 023814 (2010).
20. S.-K. Son, D. A. Telnow, and S. I. Chu, "Probing the origin of elliptical high-order harmonic generation from aligned molecules in linearly polarized laser fields," Phys. Rev. A **82**, 043829 (2010).
21. Y. Xia and A. Jaron-Becker, "Multielectron contributions in elliptically polarized high-order harmonic emission from nitrogen molecule," Opt. Lett. **39**, 1461–1464 (2014).
22. J. B. Watson, A. Sanpera, X. Chen, and K. Burnett, "Harmonic generation from a coherent superposition of states," Phys. Rev. A **53**, R1962–R1965 (1996).
23. A. Sanpera, J. B. Watson, M. Lewenstein, and K. Burnett, "Harmonic-generation control," Phys. Rev. A **54**, 4320–4326 (1996).
24. D. B. Milosevic, "Theoretical analysis of high-order harmonic generation from a coherent superposition of states," J. Opt. Soc. Am. B **23**, 308–317 (2006).
25. D. B. Milosevic, "High-energy stimulated emission from plasma ablation pumped by resonant high-order harmonic generation," J. Phys. B **40**, 3367–3376 (2007).
26. D. B. Milosevic, "Resonant high-order harmonic generation from plasma ablation: Laser intensity dependence of the harmonic intensity and phase," Phys. Rev. A **81**, 023802 (2010).
27. V. Strelkov, "Role of Autoionizing State in Resonant High-Order Harmonic Generation and Attosecond Pulse Production," Phys. Rev. Lett. **104**, 123901 (2010).
28. R. Ganeev, M. Suzuki, M. Baba, and H. Kuroda, "High-order harmonic generation from boron plasma in the extreme-ultraviolet range," Opt. Lett. **30**, 768 (2005).
29. B. R. Mollow, "Power Spectrum of Light Scattered by Two-Level Systems," Phys. Rev. **188**, 1969–1975 (1969).
30. T. Zuo, S. Chelkowski, and A. D. Bandrauk, "Harmonic generation by the H_2^+ molecular ion in intense laser fields," Phys. Rev. A **48**, 3837–3844 (1993).
31. T. Zuo and A. D. Bandrauk, "Charge-resonance-enhanced ionization of diatomic molecular ions by intense lasers," Phys. Rev. A **52**, R2511–R2514 (1995).
32. A. Becker and F. H. M. Faisal, "Intense-field many-body S-Matrix theory," J. Phys. B **38**, R1–R56 (2005).
33. A. Etches and L. B. Madsen,"Extending the strong-eld approximation of high-order harmonic generation to polar molecules: gating mechanisms and extension of the harmonic cutoff," J. Phys. B **43** 155602 (2010).
34. M. F. Ciappina, A. Becker and A. Jaron-Becker,"High-order harmonic generation in fullerenes with icosahedral symmetry," Phys. Rev. A **78**, 063405 (2008).
35. C. Figueira de Morisson Faria, "One and two-center processes in high-order harmonic generation in diatomic molecules: Influence of the internuclear separation," Laser Phys. **19**, 797–804 (2009).
36. D. B. Milosevic , E. Hasovic, S. Odzak, M. Busuladzic, A. Gazibegovic-Busuladzic, and W. Becker, "New results in above-threshold ionization and high-order harmonic generation of atomic and molecular systems," Laser Phys. **19**, 185–190 (2009).
37. C. A. Ullrich, *Time-dependent density-functional theory: concepts and applications* (Oxford University Press, 2012).
38. E. Penka Fowe and Andre D. Bandrauk, "Nonlinear time-dependent density-functional-theory study of ionization and harmonic generation in CO_2 by ultrashort intense laser pulses: orientational effects," Phys. Rev. A **81**, 023411 (2010).
39. D. Dundas, "Multielectron effects in high harmonic generation in N_2 and benzene: Simulation using a non-adiabatic quantum molecular dynamics approach for laser-molecule interactions," J. Chem. Phys. **136**, 194303 (2012).
40. E. Luppi and M. Head-Gordon, "Computation of high-harmonic generation spectra of H_2 And N_2 in intense

#255420 Received 9 Dec 2015; revised 23 Jan 2016; accepted 26 Jan 2016; published 25 Feb 2016

laser pulses using quantum chemistry methods and time-dependent density functional theory," Mol. Phys. **110** 909–923 (2012).
41. R. van Leeuwen and E. J. Baerends, "Exchange-correlation potential with correct asymptotic behavior," Phys. Rev. A **49**, 2421–2431 (1994).
42. D. Baykusheva, P. M. Kraus, S. B. Zhang, N. Rohringer, and H. J. Wörner, "The sensitivities of high-harmonic generation and strong-field ionization to coupled electronic and nuclear dynamics," Faraday Discuss. **171**, 113–132 (2014).
43. H. J. Wörner, J. B. Bertrand, B. Fabre, J. Hiquet, H. Ruf, A. A. Dubrouil, S. Patchkovskii, M. Spanner, Y. Mairesse, V. Blanchet, E. Mvel, E. Constant, P. B. Corkum, and D. M. Villeneuve, "Conical intersection dynamics in NO_2 probed by homodyne high-harmonic spectroscopy," Science **334**, 208-212 (2011).

The nonperturbative interaction between atoms, molecules or solids and an intense laser fields results, among other phenomena, in high-order harmonic generation (HHG) [1,2]. In one of the most extreme cases, the upconversion of the fundamental driver frequency via HHG has recently led to the generation of coherent soft X-ray laser light [3]. The radiation is emitted as isolated bursts or in trains of attosecond pulses of light [4–7]. While the process is often studied in neutral atoms, more recently HHG generation from plasma containing atomic ions has been observed as well [8,9]. HHG process has been also proposed as a spectroscopic tool to image static and dynamic properties of molecules [10–16]. The analysis of HHG itself as well as its spectroscopic applications is often based on approximations such as the semiclassical treatment of the electron-field interaction and the single-active electron approximation. Accordingly, our basic understanding of HHG relies on the three-step model [17], in which the electron is first tunnel ionized, then driven by the field and finally recombines with the parent ion leading to the emission of light in a form of integer harmonics of the fundamental driver laser frequency. In recent years it however has been shown that, in particular in the case of molecules, the generated harmonic spectra often incorporate more features than predicted by this basic picture. For example, the relevance of multi-electron contributions for the interpretation of experimental data on the ellipticity of high-order harmonics from nitrogen molecules has been demonstrated [18–21]. This results from the fact that in molecules often there are several orbitals energetically close together in the neutral as well as the cation. Therefore, the emission of electrons from different orbitals or the coupling between different orbitals becomes more likely. In particular, if the laser field is resonant with a transition, a coherent superposition of states can be formed during the pulse. It is known from atomic and model studies that resonant HHG and HHG from a coherent superposition of states can affect the spectrum [22–27], as resonant harmonics may form their own plateau and cutoff, the temporal characteristics of the corresponding harmonics may change and even transitions via autoionizing states may be involved. Besides fundamental interest, such studies are also motivated by experimental studies on plasma ablation [28].

In this article we predict and analyze the presence of sidebands of the 'usual' odd harmonics due to the interaction of molecules with intense laser radiation. They appear when the driver wavelength is tuned to the transition between one of the inner valence orbitals and a hole in the highest occupied molecular orbital (HOMO) and is, hence, most prominent in the interaction of open shell molecules with intense laser radiation. The mechanism is analogous to that responsible for Mollow sidebands in quantum optics [29]. Similar sidebands have been identified before for the HOMO-LUMO transition in the simplest molecular ion, H_2^+, in the regime of charge resonance enhanced ionization at large internuclear distances [30,31]. According to the results of our calculations the phenomenon is however more general and occurs for many open shell molecules at equilibrium geometry. In particular, in the general case charge resonance effects [31] do not have to be induced and the phenomenon appears due to straightforward coupling of orbitals of different types of symmetry. Furthermore, the coupling of the orbitals and related transition introduces an additional time scale, that is related to a nonadiabatic dynamics and induces dynamical localization of the electron within the molecule. All of the results

#255420 Received 9 Dec 2015; revised 23 Jan 2016; accepted 26 Jan 2016; published 25 Feb 2016

are not described by the standard 'strong field approximation' approaches for multi-electron molecular systems [14, 18, 32–36] and show how excitations during the HHG process can lead to nonadiabatic internal dynamics which strongly affects the HHG spectra.

In order to calculate the response of a molecule, including multi-electron effects, to an intense laser field, we make use of the time-dependent density functional theory (TDDFT). In the past this theoretical approach has been applied successfully to determine optical properties of molecules and clusters [37] as well as high-order harmonic generation [38–40]. It is based on a solution of the Kohn-Sham equations:

$$i\frac{\partial}{\partial t}\phi_k(\mathbf{r},t) = -\nabla^2\phi_k(\mathbf{r},t) + (V_{KS}[\rho(\mathbf{r},t)] + U(\mathbf{r},t))\phi(\mathbf{r},t) \quad (1)$$

where

$$\rho(\mathbf{r},t) = \sum_k \phi_k^*(\mathbf{r},t)\phi_k(\mathbf{r},t) \quad (2)$$

is the density of the non-interacting particles, ϕ_k are the so-called Kohn-Sham orbitals, V_{KS} contains correlation and exchange interactions, and $U(t)$ denotes the interaction of the Kohn-Sham orbitals with the external laser field. In the present calculations we have implemented the adiabatic local density approximation and the so called LB94 functional [41]. We have further used the approximation of Linear Combination of Atomic Orbitals for Molecular Orbitals (LCAO-MO) to represent the molecular wavefunction. In our application the Kohn-Sham equations are solved on a space-time grid for the interaction of the molecule, initially in its ground state, with an intense short laser pulse. The space-time grid had a time step size of 0.03 a.u. and a grid step size of 0.3 a.u.

In Fig. 1 we present a comparison of HHG spectra with (a) and without (b) the presence of sidebands. In the corresponding calculations we have considered the nitrogen molecular ion aligned parallel (a) and perpendicular (b) to the polarization vector of the electric field of a laser at 400 nm wavelength and an intensity of 2×10^{14} W/cm^2. The pulse length was 15 fs and the pulse shape trapezoidal. While the spectrum for the perpendicularly aligned molecular ion shows the traditional spectrum consisting of odd harmonics only (b), there are first and second order sidebands for each of the harmonics when the molecular ion is aligned along the polarization axis of the laser field (a).

The sidebands appear in between harmonic frequencies and may be also termed "fractional" harmonics. For the present laser parameters they are related to the transition between HOMO-2 (σ_u, E = -0.8799 a.u.) to HOMO (σ_g, E = -0.7763 a.u.) in this open shell molecule, which are approximately separated by the energy of a single 400 nm photon. The intensity of the sidebands is surprisingly high, which can be attributed to a rather significant transition dipole matrix element describing the coupling between these two molecular states. The mechanism responsible for the sidebands is analogous to that for Mollow sidebands in quantum optics [29]. In the insets on the right we present enlarged views of a part of the spectra. This clearly shows the relation between the separation of the first and second order sideband peaks in the spectrum and the Rabi transition frequency $\Omega_r = \mathbf{d_{i,j}} \cdot \mathbf{E}$, where $\mathbf{d_{i,j}}$ and $\mathbf{E}$ are correspondingly the transition matrix element for transition between states i and j, and the electric field.

The close relation of the present sideband structure to Mollow sidebands, known in quantum optics, is supported by the results presented in Fig. 2. In that Figure we present the dependence of the displacement of the first (solid line with circles) and the second-order (dashed line with squares) sidebands of the 9th harmonic in N_2^+, aligned parallel to the polarization axis, on the electric field strength. The displacement is determined as half of the energy difference between the right and the left sideband of the harmonic. The displacements of the sidebands scales linearly with the electric field strength and are in agreement with the (perturbative) Rabi frequency of the corresponding transition (solid and dashed lines with stars). Thus, the peak positions of

#255420 Received 9 Dec 2015; revised 23 Jan 2016; accepted 26 Jan 2016; published 25 Feb 2016

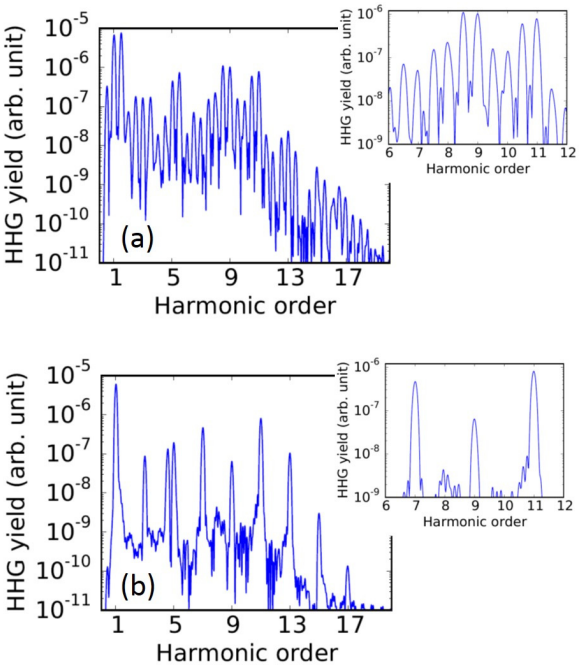

Fig. 1. High harmonic spectra of N_2^+, aligned parallel (a) and perpendicular (b) to the polarization axis of a 15 fs laser pulse at 400 nm and 2×10^{14} W/cm^2. The insets show an enlarged view of part of the spectrum, which clearly exhibit the first and second order Mollow sidebands displaced by the Rabi frequency Ω_r and $2\Omega_r$ from the odd harmonics for the aligned molecules (panel a).

the sidebands in the present results show indeed the same intensity dependence as the Mollow sidebands.

The results in Fig. 1 involve the transition between the same type of orbitals as in the previously studied case of H_2^+ [30]. However, in the previous study the sidebands occurred for the interaction of the molecular ion at larger internuclear distances, in the regime of charge resonance enhanced ionization [31]. In contrast, here the effect shows up for the interaction of the molecular ion with the field at equilibrium distance showing that the phenomenon is more general than considered before.

Mollow sidebands in high harmonic generation have so far been predicted for the coupling between orbitals of σ-symmetry only. However, in general, the phenomenon appears for the coupling between molecular orbitals of different type of symmetry as well. Since the symmetry of the orbitals governs the alignment dependence of the transition matrix element, the strengths of the respective fractional harmonics depends on the alignment between the molecular axis with respect to the polarization vector. For example, fractional harmonics due to the coupling between orbitals of π_u- (HOMO-1) and σ_g-symmetry (HOMO) in N_2^+ are induced for the interaction with a 800 nm laser pulse and perpendicular alignment of the molecule. The respective results of our calculations for the HHG spectrum in Fig. 3 clearly reveal the occurrence of the Mollow sidebands at these parameters. We may note parenthetically that for these laser parameters there is no coupling induced and, hence, no sidebands are observed for the molecular ion aligned along the polarization axis (not shown).

The strong coupling between the orbitals does not only leave its footprints in the high har-

#255420 Received 9 Dec 2015; revised 23 Jan 2016; accepted 26 Jan 2016; published 25 Feb 2016

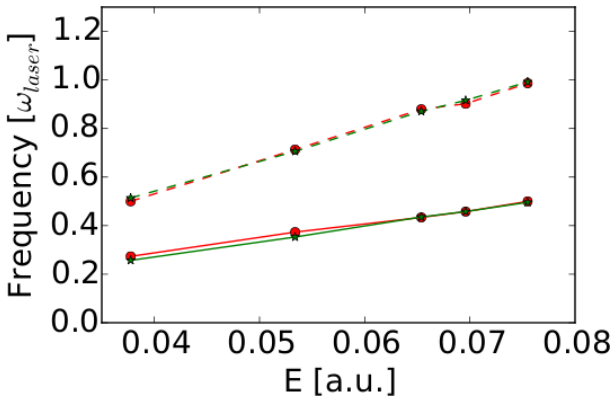

Fig. 2. Shift of the first (red solid line with circles) and second-order (red dashed line with circles) Mollow sidebands for the 9th harmonic in N_2^+, aligned parallel to the polarization direction, as function of the electric field strength. Also shown is the Rabi frequency (green solid line with stars) and twice the Rabi frequency (green dashed line with stars) for the transition between HOMO-2 (σ_u) and HOMO (σ_g). Other laser parameters are the same as in Fig. 1.

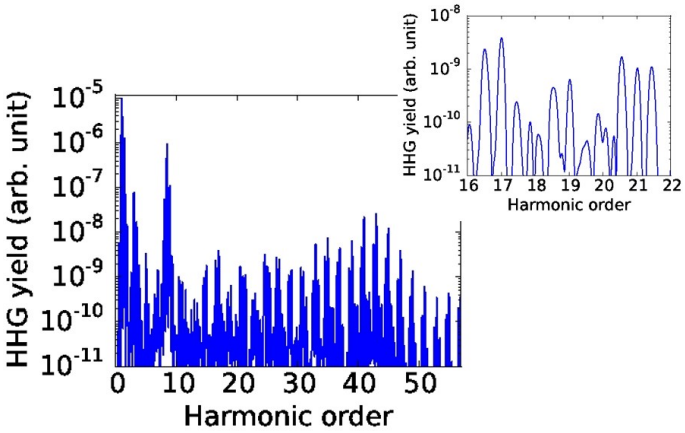

Fig. 3. High harmonic spectrum of N_2^+ aligned perpendicular to the polarization axis of a 60 fs laser pulse at 800 nm and 2×10^{14} W/cm^2. The inset provides an enlarged view of part of the spectrum.

monic spectra, but does strongly influence the dynamics of the electron density. More specifically, the emergence of sidebands comes along with profound variation of the electron dynamics inside the molecule as well as during its excursion in the continuum throughout the harmonic generation process. Firstly, the molecular orbital coupling leads to a laser induced nonadiabatic electron dynamics in the molecule, where the electron instead of directly following the changes in the oscillating electric field experiences lags and dwells at one of the nucleus for longer than a half period of the laser field cycle. The time scale of the corresponding localization of the electron is governed, as the location of the fractional harmonics in the spectrum, by the transition frequency, i.e. Rabi frequency, and can therefore in principle be controlled via the laser parameters. This nonadiabatic dynamics can be visualized in our calculations via the difference of the time-dependent total density of the propagated molecular wavepacket and the initial total

#255420 Received 9 Dec 2015; revised 23 Jan 2016; accepted 26 Jan 2016; published 25 Feb 2016

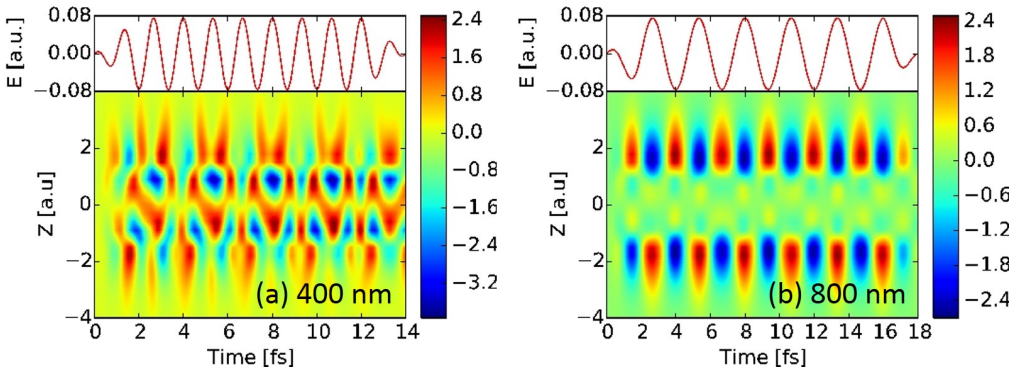

Fig. 4. Difference between the full time-dependent electron density of N_2^+, aligned along the polarization axis, and the initial electron density as a function of time and the position along the molecular axis. The densities are integrated over the spatial dimensions transversal to the molecular axis. Laser parameters as in Fig. 1.

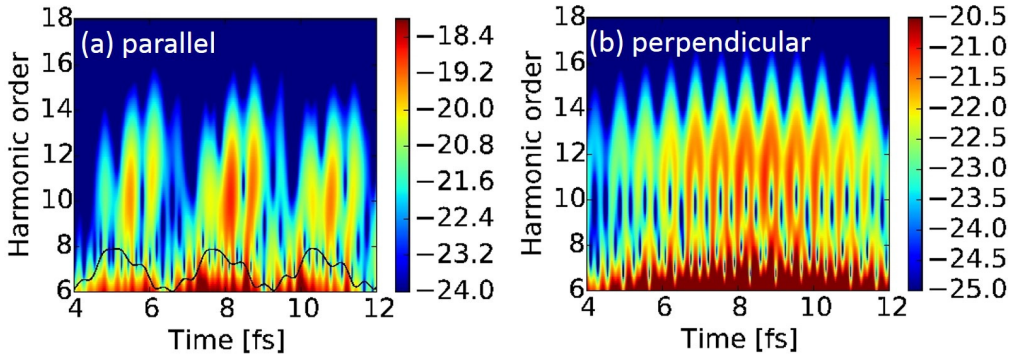

Fig. 5. Wavelet analysis of high harmonic generation in N_2^+ aligned along (a) and perpendicular to (b) the polarization direction. Laser parameters are the same as in Fig. 1.

electron density. After integration over the two spatial dimensions transversal to the molecular axis, we present the resulting total density difference, $\rho(z,t) - \rho(z,t_0)$, for N_2^+ as a function of the electron position along the internuclear axis and as a function of time in Fig. 4. The laser parameters and the orientation of the molecular axis (along the electric field vector) are the same as for the results in Fig. 1. For the purpose of comparison the electric field is shown in an inset at the top of each panel. We present changes in the density difference for the case where coupling and nonadiabatic dynamics is present (a) and for the case without coupling where one can observe, typical, adiabatic dynamics (b).

The result in Fig. 4(a) clearly shows that in the Rabi flopping regime the electron density does not swap adiabatically from one side of the molecular ion to the other every half cycle of the electric field. Instead, dynamical localization islands can be observed along the internuclear axis. However, also the electron density localized at nuclei shows nonadiabatic behavior. In contrast for adiabatic case (b) one can typically observe changes in electron density primarily around the nuclei. The frequency of the associated nonadiabatic oscillation is estimated to be approximately equal to the Rabi frequency of the transition between the states.

This nonadiabatic electron dynamics in the molecule further leads to modifications of the traditional semiclassical picture of HHG, as can be seen from the time frequency analysis in

#255420 Received 9 Dec 2015; revised 23 Jan 2016; accepted 26 Jan 2016; published 25 Feb 2016

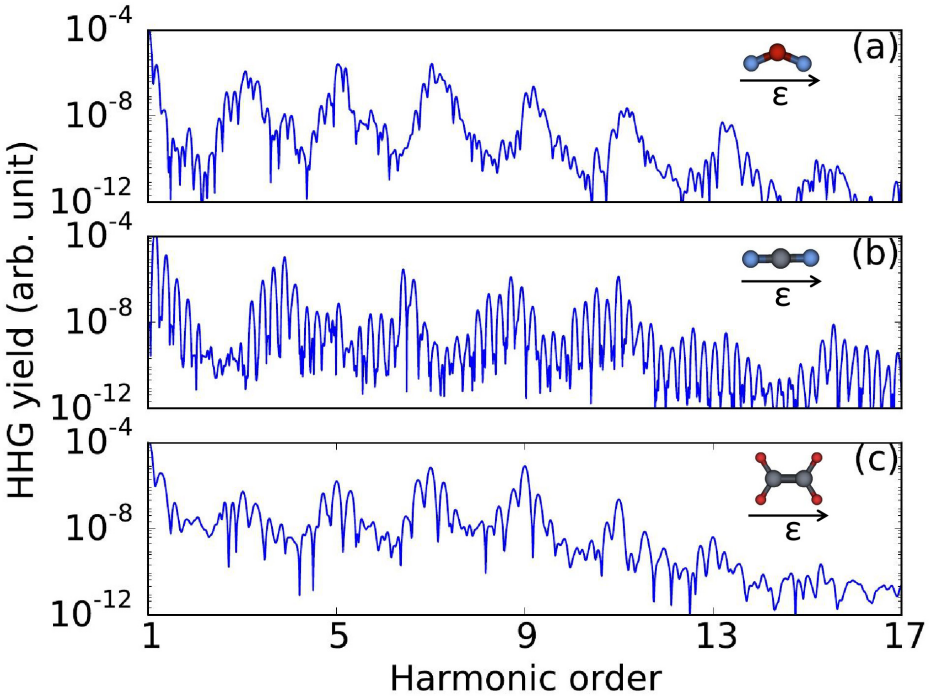

Fig. 6. High harmonic spectra showing fractional harmonics for (a) NO_2 at 400 nm, 10^{14} W/cm^2, and 40 fs pulse length, (b) CO_2^+ at 350 nm, 10^{14} W/cm^2 and 34 fs, and (c) $C_2H_4^+$ at 400 nm, 10^{14} W/cm^2 and 18 fs.

Fig. 5. Wavelet analysis has been performed using the Gaussian window with the width equal to 3 harmonic orders, using the following formula,

$$d(\omega,t) = \int d(\tau)\exp(-(\tau-t)^2/2\sigma^2)\exp(-i\omega\tau)d\tau. \quad (3)$$

In contrast to the typical wavelet analysis for high harmonic generation, which exhibits the return of the electron and harmonic emission via short and long trajectories, shown for comparison in Fig. 5 (b), the generation of the frequencies in the harmonic spectrum as a function of time related to fractional harmonics becomes more complex (see panel a). Obviously, any interpretation in terms of classical paths becomes cumbersome in this case. Instead, the time-frequency pattern is modulated by the nonadiabatic dynamics and temporal variation of the electron localization inside the molecule and, not surprisingly, shows an additional oscillating variation of the pattern with the time scale related to the Rabi frequency for transition between HOMO and HOMO-2 in the nitrogen molecular ion. For illustration of the time scale in Fig. 5 (a) the calculated HOMO population is shown superimposed over the lower part of spectrum.

Before concluding, we emphasize that the present findings are not restricted to the nitrogen molecular ion. Indeed, from the results of our calculations we observe the appearance of fractional harmonics in other larger open shell molecules as well. In Fig. 6 we present examples of harmonic spectra for the neutral triatomic open shell molecule NO_2 (a), the triatomic open shell molecular ion CO_2^+ (b) and the polyatomic molecular ion $C_2H_4^+$ (c). For each of these molecules the Mollow sidebands can be induced using wavelengths around 400 nm between different type

#255420 Received 9 Dec 2015; revised 23 Jan 2016; accepted 26 Jan 2016; published 25 Feb 2016

of orbitals: $6a_1$ (HOMO, E=-0.2016a.u.) - $4b_2$ (HOMO-1, E=-0.3136a.u.) (NO_2), $1\pi_g$ (HOMO, E=-0.8208 a.u.) - $1\pi_u$ (HOMO-2, E=-0.0.9633 a.u.) (CO_2^+), $1b_{3g}$ (HOMO-1, E=-0.6042 a.u.) - $1b_{2u}$ (HOMO-3, E=-0.7195 a.u.) ($C_2H_4^+$). The orientation of the molecule versus the polarization direction is shown in inserts in Fig. 6. In each case the harmonic spectrum has been obtained for the molecule in its equilibrium configuration. The coupling between the orbitals is strongest in CO_2^+, leading to the appearance of strong sidebands, while the transition between the orbitals is weakest for NO_2. Therefore, in the latter case the sidebands do not occur as separate peaks in the spectrum, but in contrast rather lead to a broadening of each of the odd harmonic peaks.

Finally, we may note that the present results are based on a microscopic study of molecular high-order harmonic generation. Inclusion of macroscopic effects (focal averaging and propagation), which are sometimes important for the analysis of experimental data, are very challenging for theoretical analysis of molecular high-order harmonic generation. However, the results presented in Fig. 2 provide us with the opportunity to comment on the effect of intensity averaging. As discussed above, the position of the sidebands scales linearly with the electric field strength. On the other hand, high-order harmonic generation is a strongly nonlinear process in itself. Therefore, small intensity variations in the focal averaging will lead to a drastic reduction of the harmonic yield, while the position of the sidebands varies slightly only. We may therefore expect that an intensity average will not affect the present results much. Conclusions about propagation effects cannot be done based on the present results and are beyond the scope of the present ab-initio studies.

In conclusion, we have shown that Mollow sidebands occur in high harmonic spectra of open shell molecules at equilibrium geometries. The sidebands are due to a driving laser induced one-photon coupling (Rabi flopping) between one of the inner valence orbitals and the HOMO. The phenomenon is found and illustrated for parallel as well as perpendicular transitions, di-, tri- and polyatomic molecules. Moreover we illustrate the coupling of different type of orbitals, and different orientations of the molecule. Thus, it is shown that Mollow sidebands are much more general than the previously studied case of stretched H_2^+ in the regime of charge resonance enhanced ionization. Furthermore, the time-dependent electron density and the time-frequency analysis have shown that the appearance of the sidebands comes along with a nonadiabatic electron dynamics and localization in the molecule as well as a breakdown of the traditional semiclassical picture of high harmonic generation and a description using strong field approximation [14, 18, 32–36].

Presented results represent a novel interesting property of HHG for open shell multi-electron molecules. Experimental studies and corresponding measurements may provide information about dipole transition matrix elements. In addition, the effect can also modify HHG based dynamical imaging of the chemical reactions [15], recently performed for open shell molecules [42, 43]. Many interesting chemical reactions studied vigorously due to their applications and relevance for atmospheric, combustion, polymerization research as well as plasma chemistry and biochemistry, contain free radicals which are open shell molecules and can be considered for generation of Mollow sidebands.

Acknowledgments

This work was supported via grants from the U.S. National Science Foundation (NSF) (Grant No. PHY-1068706 and Grant No. PHY-1125844). This work utilized the Janus supercomputer, which is supported by the National Science Foundation (NSF) (Grant No. CNS-08217994) and the University of Colorado, Boulder. This work also used the Extreme Science and Engineering Discovery Environment (XSEDE), which is supported by National Science Foundation (NSF) (Grant No. ACI-1053575).

#255420 Received 9 Dec 2015; revised 23 Jan 2016; accepted 26 Jan 2016; published 25 Feb 2016